Ultrafast Exciton Formation at the ZnO$(10\bar{1}0)$ Surface

J.-C. Deinert,* D. Wegkamp, M. Meyer, C. Richter, M. Wolf, and J. Stähler
Fritz-Haber-Institut der Max-Planck-Gesellschaft, Abteilung Physikalische Chemie, Faradayweg 4-6, 14195 Berlin, Germany
(Received 28 March 2014; published 30 July 2014)

We study the ultrafast quasiparticle dynamics in and below the ZnO conduction band using femtosecond time-resolved two-photon photoelectron spectroscopy. Above band gap excitation causes hot electron relaxation by electron-phonon scattering down to the Fermi level E_F followed by ultrafast (200 fs) formation of a surface exciton (SX). Transient screening of the Coulomb interaction reduces the SX formation probability at high excitation densities near the Mott limit. Located just below the surface, the SX are stable with regard to hydrogen-induced work function modifications and thus the ideal prerequisite for resonant energy transfer applications.

DOI: 10.1103/PhysRevLett.113.057602 PACS numbers: 79.60.Bm, 78.47.J-, 73.20.Mf, 73.20.At

The technological importance of zinc oxide (ZnO) originates from its large direct band gap (~3.4 eV) and high bulk exciton binding energy (60 meV) [1], which make it a promising candidate for optoelectronic applications, using ZnO nanoparticles [2–4], epilayers [4], and hybrid organic-inorganic systems [3,5,6]. In this context, the optical and electronic properties of ZnO *surfaces* naturally play a significant role with regard to electronic and excitonic coupling with other materials, e.g., organic dye molecules. As dipole-dipole coupling is highly distance dependent [7], the rates for Förster resonance energy transfer (FRET) between different materials depend strongly on the presence of exciton dead layers at the surface [8–10] or, on the contrary, the existence of surface excitons. The latter are a dominant species in photoluminescence (PL) studies of different types of ZnO nanostructures due to the comparably large surface-to-bulk ratio [2,3,11,12]. Despite the great scientific attention, detailed understanding of this technologically highly important species is still missing, as the systematic modification and characterization of nanoparticle surfaces is very challenging. Because of the lack of surface sensitivity of optical probes and PL, SX could only once be identified at a ZnO *single crystal* surface [13]. However, as the sample had been exposed to air, the surface condition was rather undefined. Neither observation nor systematic characterization of SX under ultrahigh vacuum (UHV) conditions, which provide reproducible surfaces at the nanoscale level [1,14], is known to date, and thus the origin and character of this very relevant species remains vague.

In this Letter, we use femtosecond (fs) time-resolved two-photon photoelectron (2PPE) spectroscopy to investigate the ultrafast carrier and exciton dynamics at the single crystal ZnO$(10\bar{1}0)$ surface under well-defined UHV conditions. Because of the intrinsic surface sensitivity of this technique we are able to observe the ultrafast relaxation of hot electrons in the conduction band and the subsequent formation of an excitonic state near the surface on subpicosecond time scales. High excitation densities near the Mott limit enhance the screening of the electron-hole (e-h) Coulomb interaction and thus reduce the formation probability of this state. Remarkably, even strong modification of the (static) surface charge density by hydrogen termination does *not* change the population dynamics of the SX, strongly suggesting that the exciton is localized in the *sub*surface region. This adjacence of the exciton to the surface (1–2 nm) combined with its stability with respect to surface modification demonstrates its direct relevance for applications of ZnO involving resonant energy transfer.

Figure 1(a) depicts the principle of time-resolved 2PPE spectroscopy. A first laser pulse initiates nonequilibrium dynamics by excitation of electrons from the valence band (VB) into normally unoccupied states in the conduction band (CB). A second laser pulse subsequently photoemits the excited electron population. The temporal evolution is monitored by variation of the time delay between pump and probe pulse [15]. The photoelectrons were detected using a hemispherical electron energy analyzer (PHOIBOS 100) held at a fixed bias voltage (1.5 V) with respect to the sample. Photoelectron (PE) spectra are referenced to the, *in situ* measured, tantalum sample holder Fermi energy E_F, which was in electrical contact with the sample surface.

We investigated three different hydrothermally grown ZnO single crystals (Mateck) and found no quantitative differences. Their nonpolar, mixed-terminated $(10\bar{1}0)$ surfaces were prepared by Ar^+ sputtering and annealing cycles ($T_{max} = 850$ K) under UHV conditions ($p_{base} = 1 \times 10^{-10}$ mbar). The VB maximum remains unchanged at $E - E_F = -3.18(6)$ eV for different types of preparations using oxygen background pressures up to 10^{-6} mbar (not shown). Neither charging, nor surface photovoltage effects have been observed [16]. Unless otherwise stated, experiments were performed at $T = 100$ K. Incident fluences between 10 and 35 $\mu J/cm^2$ translate to maximum excitation densities of $1.45–5.22 \times 10^{18}$ cm^{-3}, which is below or close to the Mott limit [17]. Hydrogen termination of the surface was achieved by background dosing of H_2 [18].

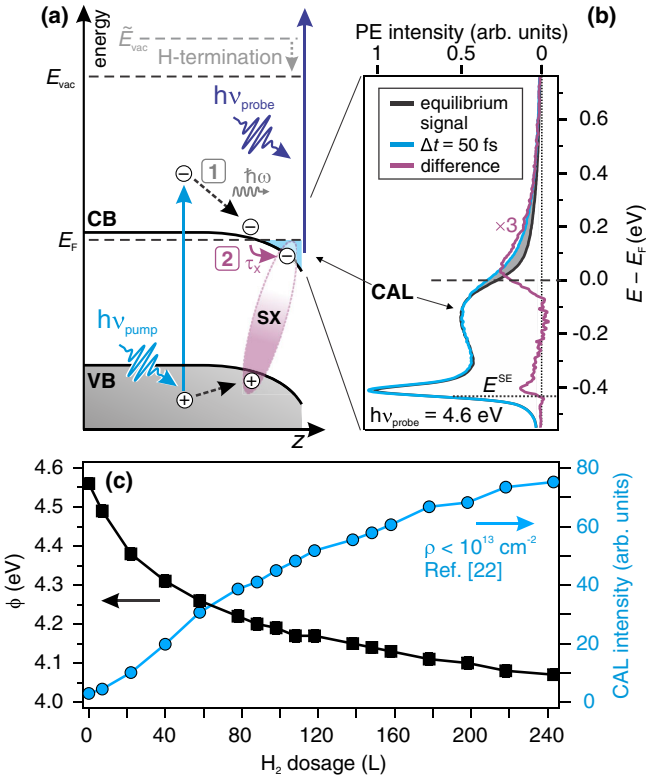

FIG. 1 (color online). (a) 2PPE principle and relevant processes. Photoexcited ($h\nu_{pump}$) electrons relax by electron-phonon scattering (1) and exciton formation (2), which is probed by a time-delayed laser pulse ($h\nu_{probe}$) in photoemission. (b) Exemplary photoelectron spectrum of the hydrogen-terminated ZnO surface (black). The low-energy cutoff $E^{SE} = \Phi - h\nu_{probe}$ is a measure of the work function; the intensity below E_F results from the CAL at the surface. Above band gap excitation leads to additional 2PPE intensity around E_F (blue). Subtraction of the equilibrium background signal yields the pump-induced spectrum (purple). (c) Impact of hydrogen termination on sample work function and CAL intensity.

Exposure of a semiconductor surface to an electron donor (like hydrogen) can lead to downward surface band bending (SBB). In the case of the intrinsically n-doped ZnO, this leads to the formation of a few 10 Å thick charge accumulation layers (CAL) at the $(10\bar{1}0)$ surface [19–21] with a maximum surface charge density of 10^{13} cm^{-2} [22]. We monitor the CAL formation by (1) the occurrence of photoelectron intensity directly below E_F as shown in Fig. 1(b) and (2) by a reduction of the sample work function that is correlated with the surface band bending as sketched in Fig. 1(a). Figure 1(c) shows that increasing H_2 exposure leads, in agreement with literature [22], to an increasing CAL intensity (blue curve) [23], which is accompanied by a work function decrease that saturates at $\Delta\Phi_{max} = -0.6$ eV. This change of the surface dipole is a result of the electron donor character of the hydrogen, leaving the positively charged ion at the surface. Directly after preparation of a pristine ZnO surface, a slight but continuous increase of CAL intensity going along with a work function reduction of several 10 meV is always observed due to the inevitable H_2 background even in a UHV environment (< 0.1 L/h). In order to stabilize the PE signal and to reduce the work function, we exposed the sample (unless otherwise stated) to 6 L of H_2 before experiments, which corresponds, based on Ref. [22], to a charge density in the CAL on the order of 10^{18} cm^{-3} and a termination of surface oxygen of only a few percent.

Figure 2(a) shows the *photoinduced* 2PPE intensity, i.e., after subtraction of the equilibrium background [cf. Fig. 1(b)], in false colors as a function of pump-probe delay and energy with respect to E_F. Photoexcitation below the Mott limit (max. excitation density 1.45×10^{18} cm^{-3}) launches fast dynamics at high energies that significantly slow down for $E - E_F < 0.2$ eV. Note that experiments at even lower excitation densities expose qualitatively similar dynamics (not shown) [24]. Exemplary cross correlation (XC) traces are depicted in Fig. 2(b) (circles), which can be fitted (solid lines) using bi-exponential decays convolved with the laser pulses' cross correlation (dashed). The fast time constant of this empirical fit can be related to the hot electron relaxation time at the respective energy. We performed similar experiments for temperatures between 50 and 300 K, the results of which are presented in Fig. 2(c). In agreement with previous 2PPE autocorrelation measurements [25] and theoretical work [26], we find extremely fast electron relaxation for carriers above the bulk conduction band minimum (CBM) [$\tau = 20$–40 fs, gray shaded area in Fig. 2(c)]. These fast relaxation times compared to hot electrons in metals [27] can be explained by the reduced screening in the semiconductor. They result from scattering with optical phonons and are therefore independent of temperature in the investigated region ($k_BT < 26$ meV). Theory [26] predicts a slowing down of the electron relaxation in the bulk when approaching the CBM [dashed line in Fig. 2(c)], because fewer efficient scattering channels require more scattering events for the same energy loss. In the present experiment, at the $ZnO(10\bar{1}0)$ surface, such a "phonon bottleneck" does not occur, as the downward surface band bending provides density of states (DOS) down to E_F [see inset in Fig. 2(c)].

The dynamics *below* E_F differ significantly from the ones above. Integration of the 2PPE intensity yields the diamond-shaped markers in Fig. 2(b). They display an initial drop of intensity, which is due to bleaching of the CAL by $h\nu_{pump}$, followed by a rise up to a constant positive value. Notably, this delayed increase of pump-induced 2PPE intensity occurs *below* E_F, i.e., below the energy which defines the highest occupied electronic state in equilibrium. Consequently, $h\nu_{pump}$ must create additional states below E_F leading to an increased 2PPE signal. Such photoinduced creation of states could be caused by (i) small polaron formation, (ii) photoinduced changes of the surface electronic structure like surface photovoltage shifts, band gap renormalization, or heating or bleaching of the CAL, or (iii) exciton formation.

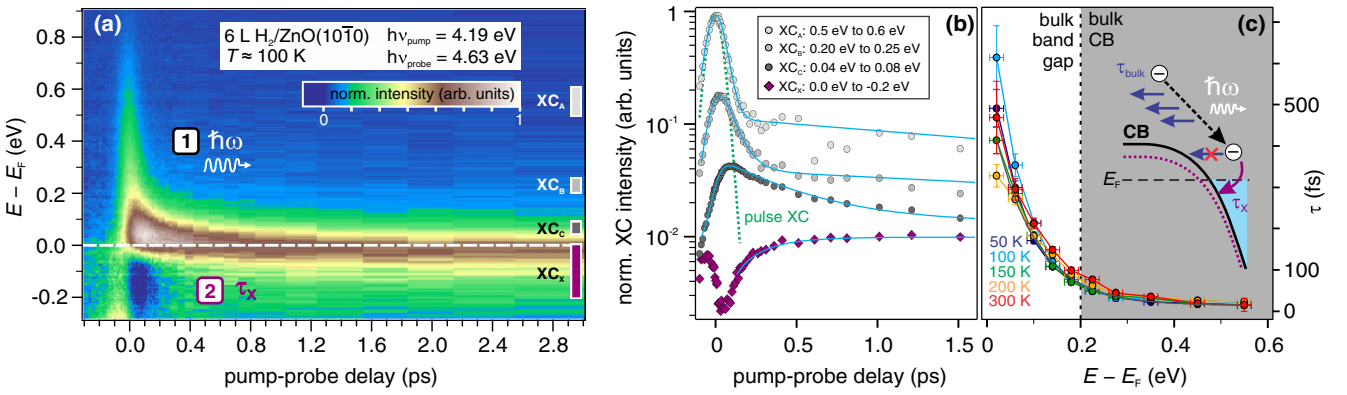

FIG. 2 (color online). (a) Ultrafast electron dynamics at the ZnO surface below the Mott limit as probed by 2PPE spectroscopy. False colors represent photoelectrons created or depleted by $h\nu_{\mathrm{pump}}$. Hot carriers in the CB relax on fs time scales by optical phonon emission. After a few 100 fs, additional electrons are verified below E_F, indicating that the surface exciton has formed. The signal at negative delays and energies results from photoelectrons with reversed excitation scheme (pumped by 4.6 eV and probed by 4.2 eV) and are a replica of the above dynamics shifted to 0.4 eV lower final state energies and evolving towards negative delays. (b) Pump and probe XC traces at indicated energies above (hot electrons) and below E_F (exciton) and the corresponding double exponential fits to the data (solid lines). The instrument response function is represented by the dashed curve. (c) Temperature dependence of the hot electron relaxation time and scheme of the different relaxation channels.

It is well known that lattice distortions stabilize the ZnO exciton and lead to its large binding energy of 60 meV [28]. The formation of *separate* polarons of electron and hole is thus unlikely. Also, no experimental evidence of small polaron formation was found by recent time-resolved THz spectroscopy studies of ZnO [29], excluding scenario (i). We tested the validity of (ii) and (iii) by a variation of the excitation density. While, in the case of (ii), photo-induced changes of the SBB and occupational changes due to laser heating should become stronger with increasing pump fluence, (iii) the probability of exciton formation should be independent of excitation density below the Mott limit, i.e., the density at which the screening of the Coulomb interaction sets in [see inset in Fig. 3(a)]. For stronger excitation the Coulomb interaction of the *e-h* pairs is reduced by the photoexcited *e-h* plasma and thus the exciton formation probability diminishes.

Figure 3(a) compares 2PPE spectra of two different excitation densities near the Mott limit of ZnO at different time delays. While the overall dynamics do not change, the intensity of the spectral signature at E_F is *reduced* by the *increase* of the excitation density. This observation unambiguously shows that (ii) photoinduced changes of SBB and CAL density cannot be the cause of the observed peak. On the contrary, the decreased intensity matches the expectations (iii) for an exciton whose formation probability is reduced by screening of the *e-h* interaction. As all of these processes must happen in the surface region [30], we conclude that the photoinduced intensity below E_F results from near surface-bound excitons (SX) with a binding energy with respect to the bulk conduction band minimum of 250 meV. It should be noted that, in the SBB picture, the local binding energy relative to the local CBM is probably smaller [cf. inset of Fig. 2(c), dotted curve]. The continuous evolution of the SX signature from the hot electron distribution is a direct consequence of the off-resonant excitation leading to carriers that relax to the band edges. The formation of SX occurs at least as fast as the observed rise time of PE intensity below E_F of 200 fs, however, these excitons are in a highly excited "hot" state that relaxes to the ground state on longer time scales [31]. Due to the limited energy resolution (45 meV) and because PES averages over the energy distribution in the SBB region, the spectral signatures of electron and exciton blend smoothly into each other [32]. As the electron of the SX energetically lies *below* the Fermi level, nonradiative decay of this excitation is strongly suppressed: Dissociation of the exciton and separation of electron and hole in defect states within the band gap usually is a prominent non-radiative decay channel for excitons. It *cannot* occur here, as most possible final states for the electron lie below E_F and are therefore occupied. The decay of the SX population can thus only happen through *e-h* pair recombination going along with luminescence or Auger-type processes, which results in the high stability of this excited state [33].

In order to test the stability of the SX, we modified the surface electronic properties by variation of the hydrogen termination. As mentioned above, this leads to a reduction of the sample work function by hundreds of meV and concurrent formation of a CAL at the surface. Such strong modification of the surface electronic structure should severely affect the formation probability of the SX if it was localized in the vacuum in front of the surface (through the modified ionization potential leading to spectral shifts) or in the first double layer (through the screening of the Coulomb interaction by the charge density in the CAL leading to a reduction of the SX intensity with

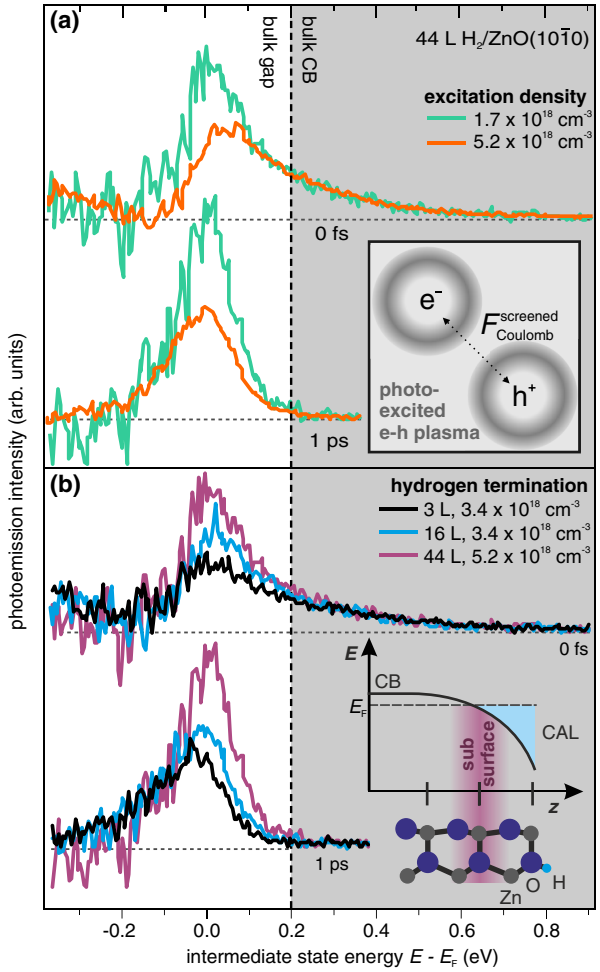

FIG. 3 (color online). 2PPE spectra for (a) different excitation densities and (b) hydrogen terminations after background subtraction and normalized to the hot electron intensity at high energies (0.4–0.6 eV) in order to compare changes relative to the single particle excitation density. (a) Stronger excitation reduces the SX formation probability due to screening of the Coulomb interaction as illustrated in the insets. (b) The SX intensity does *not* decrease with increasing H_2 termination showing localization in the subsurface region as illustrated by the inset.

increasing termination). As shown in Fig. 3(b), none of these effects occur when increasing the H_2 exposure from 3 to 44 L ($\Delta\Phi_{max} = -250$ meV). We thus conclude that the SX is localized in the subsurface region where additional static screening of the Coulomb interaction does not occur. On the contrary, increasing the hydrogen exposure by more than a factor of 10 leads to a comparably weak *increase* of the SX intensity and a weak shift to higher energies. This observation could be explained by SX localized close to hydrogen binding sites where the downward SBB is strongest and a denser CAL with increasing termination that could give the SX Mahan exciton character (see, e.g., [34]), i.e., the energetic stabilization of the CAL due to a localized hole in the VB.

In summary, we present a systematic investigation of the ultrafast electron and exciton dynamics at the ZnO(10$\bar{1}$0) surface, showing the formation of a subsurface-bound exciton on fs time scales that exhibits a very large binding energy with respect to the bulk conduction band, resulting in a remarkable stability of this feature. The study thus offers a complete and novel picture of the quasiparticle relaxation at this surface. The existence of a subsurface exciton which is stable with regard to surface modifications is of high relevance for applications of ZnO, e.g., involving FRET. The SX may dominate the dipole-dipole coupling across functional interfaces due to its adjacence to the surface, and it may even persist under non-UHV conditions.

We are grateful for stimulating discussions with T. Kampfrath, P. Rinke, and O. Hofmann at the FHI Berlin. This work was partially funded by the Deutsche Forschungsgemeinschaft through Sfb 951 and the European Union through Grant No. 280879-2 CRONOS CP-FP7.

*deinert@fhi-berlin.mpg.de

[1] C. Wöll, Prog. Surf. Sci. **82**, 55 (2007).
[2] J.-P. Richters, T. Voss, D. S. Kim, R. Scholz, and M. Zacharias, Nanotechnology **19**, 305202 (2008).
[3] M. Slootsky, X. Liu, V. M. Menon, and S. R. Forrest, Phys. Rev. Lett. **112**, 076401 (2014).
[4] C. Klingshirn, J. Fallert, H. Zhou, J. Sartor, C. Thiele, F. Maier-Flaig, D. Schneider, and H. Kalt, Phys. Status Solidi B **247**, 1424 (2010).
[5] F. Della Sala, S. Blumstengel, and F. Henneberger, Phys. Rev. Lett. **107**, 146401 (2011).
[6] Y. Xu, O. T. Hofmann, R. Schlesinger, S. Winkler, J. Frisch, J. Niederhausen, A. Vollmer, S. Blumstengel, F. Henneberger, N. Koch, P. Rinke, and M. Scheffler, Phys. Rev. Lett. **111**, 226802 (2013).
[7] T. Förster, Ann. Phys. (Berlin) **437**, 55 (1948).
[8] H.-J. Egelhaaf and D. Oelkrug, J. Cryst. Growth **161**, 190 (1996).
[9] V. A. Fonoberov and A. A. Balandin, Phys. Rev. B **70**, 195410 (2004).
[10] G. Kiliani, R. Schneider, D. Litvinov, D. Gerthsen, M. Fonin, U. Rüdiger, A. Leitenstorfer, and R. Bratschitsch, Opt. Express **19**, 1641 (2011).
[11] V. A. Fonoberov and A. A. Balandin, Appl. Phys. Lett. **85**, 5971 (2004).
[12] S. Kuehn, S. Friede, S. Sadofev, S. Blumstengel, F. Henneberger, and T. Elsaesser, Appl. Phys. Lett. **103**, 191909 (2013).
[13] V. Travnikov, A. Freiberg, and S. Savikhin, J. Lumin. **47**, 107 (1990).
[14] U. Diebold, L. V. Koplitz, and O. Dulub, Appl. Surf. Sci. **237**, 336 (2004).
[15] Laser pulses were provided by a regeneratively amplified (RegA), tuneable fs-laser (200 kHz). The frequency-doubled output of an optical parametric amplifier provided

$h\nu_{\mathrm{pump}} = 3.76$–$4.2$ eV and the third (4.65 eV) and fourth harmonic (6.2 eV) of the 800 nm RegA output were used for photoemission.

[16] As discussed further below, the observed spectral features exhibit neither fluence nor temperature dependence.

[17] Literature values for the Mott density vary between 1.5 and 6×10^{18} cm^{-3} [29,34,35]. The calculated maximum excitation densities give an upper limit for the absorption directly at the surface.

[18] The glowing filament of an ion gauge was set 15 cm in line of sight with the sample surface leading to an increased dissociation of H_2.

[19] D. Eger, A. Many, and Y. Goldstein, Surf. Sci. **58**, 18 (1976).

[20] H. Lüth, *Solid Surfaces, Interfaces and Thin Films*, edited by W. T. Rhodes, H. E. Stanley, and R. Needs (Springer, Berlin, Heidelberg, 2010).

[21] Y. Wang, B. Meyer, X. Yin, M. Kunat, D. Langenberg, F. Traeger, A. Birkner, and C. Wöll, Phys. Rev. Lett. **95**, 266104 (2005).

[22] K. Ozawa and K. Mase, Phys. Rev. B **83**, 125406 (2011).

[23] The sticking coefficient is unknown and dissociation of H_2 occurs at filaments in the chamber plays a role, which inhibits quantitative comparison of the exposures to Ref. [22].

[24] The observed dynamics thus cannot be attributed to collective phenomena of the excited *e-h* plasma like, e.g., Fermi edge singularities [36–38].

[25] W. A. Tisdale, M. Muntwiler, D. J. Norris, E. S. Aydil, and X.-Y. Zhu, J. Phys. Chem. C **112**, 14682 (2008).

[26] V. P. Zhukov, P. M. Echenique, and E. V. Chulkov, Phys. Rev. B **82**, 094302 (2010).

[27] M. Lisowski, P. Loukakos, U. Bovensiepen, J. Stähler, C. Gahl, and M. Wolf, Appl. Phys. A **78**, 165 (2004).

[28] The Coulomb attraction between electron and hole and its screening in the dielectric material determines the binding energy and localization of the exciton. In particular, in semiconductors with ionic character like TiO_2 and ZnO, the coupling of carriers and excitons to the lattice, even on ultrafast time scales, cannot be neglected [26,39,40]. This leads to a polaronic character of the exciton (relaxation of ions localizes the *e-h* pair), leading to a change of exciton binding energy due to coupling with phonons [41].

[29] E. Hendry, M. Koeberg, and M. Bonn, Phys. Rev. B **76**, 045214 (2007).

[30] The SX feature is caused by the downward SBB, which extends only 1 nm into the ZnO crystal [22]. Also, PE is only sensitive to the first few nm due to the finite mean free path of electrons in a solid.

[31] The 1*s* ground state formation of the exciton usually occurs, depending on the material, on a ps to ns time scale. [29,42,43].

[32] This is different to the SX formation at the Si(100) surface, where the exciton results from electrons and holes in the electronic surface states and not the CB and VB continuum [44] and also not comparable to the transient excitons at the Ag(111) surface, which decay on fs time scales [45].

[33] The SX population decay is slower than the 400 ps accessible in our experiment. Comparison with the results achieved by Tisdale *et al.* [25] using a 76 MHz oscillator suggests lifetimes exceeding 10 ns.

[34] A. Schleife, C. Rödl, F. Fuchs, K. Hannewald, and F. Bechstedt, Phys. Rev. Lett. **107**, 236405 (2011).

[35] M. A. M. Versteegh, T. Kuis, H. T. C. Stoof, and J. I. Dijkhuis, Phys. Rev. B **84**, 035207 (2011).

[36] R. A. Kaindl, S. Lutgen, M. Woerner, T. Elsaesser, B. Nottelmann, V. M. Axt, T. Kuhn, A. Hase, and H. Künzel, Phys. Rev. Lett. **80**, 3575 (1998).

[37] I. Perakis and T. Shahbazyan, Surf. Sci. Rep. **40**, 1 (2000).

[38] R. Huber, F. Tauser, A. Brodschelm, M. Bichler, G. Abstreiter, and A. Leitenstorfer, Nature (London) **414**, 286 (2001).

[39] L. Chiodo, J. M. Garcìa-Lastra, A. Iacomino, S. Ossicini, J. Zhao, H. Petek, and A. Rubio, Phys. Rev. B **82**, 045207 (2010).

[40] E. M. Bothschafter, A. Paarmann, E. S. Zijlstra, N. Karpowicz, M. E. Garcia, R. Kienberger, and R. Ernstorfer, Phys. Rev. Lett. **110**, 067402 (2013).

[41] H.-C. Hsu and W.-F. Hsieh, Solid State Commun. **131**, 371 (2004).

[42] S. Chatterjee, C. Ell, S. Mosor, G. Khitrova, H. M. Gibbs, W. Hoyer, M. Kira, S. W. Koch, J. P. Prineas, and H. Stolz, Phys. Rev. Lett. **92**, 067402 (2004).

[43] R. A. Kaindl, D. Hägele, M. A. Carnahan, and D. S. Chemla, Phys. Rev. B **79**, 045320 (2009).

[44] M. Weinelt, M. Kutschera, T. Fauster, and M. Rohlfing, Phys. Rev. Lett. **92**, 126801 (2004).

[45] X. Cui, C. Wang, A. Argondizzo, S. Garrett-Roe, B. Gumhalter, and H. Petek, Nat. Phys. **10**, 505 (2014).